The early prediction of lithium-ion battery remaining useful life using a novel Long Short-Term Memory network

1st Meng Zhang
Information Engineering College
Capital Normal University
Beijing, China
2191002032@cnu.edu.cn

2nd Lifeng Wu*
Beijing Key Laboratory of Electronic System Reliability Technology
Capital Normal University
Beijing, China
wulifeng@cnu.edu.cn

3rd Zhen Peng
Information Management Department
Beijing Institute of Petrochemical Technology
Beijing, China
zhenpeng@bipt.edu.cn

2021 IEEE 16th Conference on Industrial Electronics and Applications (ICIEA) | 978-1-6654-2248-2/21/$31.00 ©2021 IEEE | DOI: 10.1109/ICIEA51954.2021.9516254

***Abstract*—Accurate prediction of the lithium-ion battery remaining useful life can effectively manage the lithium-ion battery health. Using the early cycle data to predict the remaining useful life can reduce consumption and detect battery failures earlier, but it is still a great challenge due to weak and high dimensional nonlinear feature data of the early cycle. In order to solve this issue, this paper proposes a Long Short-Term Memory (LSTM) model that combines the idea of Broad Learning System (BLS), called BLS-LSTM, to accurately forecast the lithium-ion battery remaining useful life by using early cycle data. Firstly, according to the BLS idea, more effective feature nodes are obtained by performing mapping operations and enhancement operations on input features. Secondly, the characteristic nodes are input into the LSTM as new input nodes to predict the remaining useful life of the lithium-ion battery. Finally, the proposed model is validated with different early cycle data and compared with other methods. The results show that the BLS-LSTM model has better prediction performance and higher accuracy in the early prediction of the remaining useful life.**

***Index Terms*—Lithium-ion battery, Remaining useful life, Early cycle data, Long Short-Term Memory, Broad Learning System**

I. Introduction

Lithium-ion batteries are more and more widely used because of their high energy, long cycle life, and good safety performance. Therefore, it is particularly important to perform health management on lithium-ion batteries to ensure the safe and effective operation of items. The prediction of lithium-ion batteries remaining useful life (RUL) has been widely investigated [1]–[3]. Accurate RUL prediction of lithium-ion batteries using early cycle data can reduce consumption, detect battery failures earlier, and improve battery performance, which can bring new opportunities for battery production, use and optimization. However, the early cycle capacity degradation is not obvious, there is less effective information in the feature data, and the operating status of lithium-ion battery is affected by different operating conditions, such as current, voltage, temperature, discharge rate. Therefore, it is still a challenging task to accurately predict RUL of lithium-ion batteries with early cycle data.

Generally, model-based methods and data-driven methods are two common methods of RUL prediction [4], [5]. Model-based methods usually include electrochemical model, equivalent circuit model and empirical model. The electrochemical model establishes an accurate and reliable model by studying the physical and chemical phenomena in the process of battery charging and discharging and the degradation factors that affect battery performance. Equivalent circuit model is a circuit model built by circuit devices to equivalent the internal degradation characteristics of the battery. The empirical model reflects the law of battery degradation according to the state characteristics in the process of battery degradation. The filtering methods are common empirical models. Luis et al. [6] proposed an online monitoring method based on Gaussian Process filtering for the state of charge of lithium-ion batteries in electric vehicles. Li et al. [7] proposed an adaptive odorless Kalman filter to estimate the state of charge of battery and concentration and potentials of lithium-ion. Zhang et al. [8] proposed an nonlinear-drifted fractional Brownian motion with multiple hidden state variables RUL forecast method. Ma et al. [9] proposed a nonlinear and non-Gaussian systems lithium-ion batteries remaining useful life prediction method based on Gaussian-Hermite particle filter. Yang et al. [10] studied the electrical characteristics of lithium-ion capacitors and established a corresponding equivalent circuit model. On this basis, they proposed an adaptive square root cubature Kalman Filter, using a variable forgetting factor recursive least square to realize the charge estimation state of each sampling step. Zhang et al. [11] proposed a Box-Cox transformation and Monte Carlo simulation RUL prediction method that can predict RUL independently of offline training data. Zhang et al. [12] proposed an unscented particle filter algorithm to improve the remaining useful life prediction accuracy, which is based on linear optimal combination resampling. Yang et al. [13] established a semi-empirical model based on the relationship

National Natural Science Foundation of China (No.61873175), and Academy for Multidisciplinary Studies of Capital Normal University, and Youth Innovative Research Team of Capital Normal University.

between the Coulomb efficiency and the lithium inventory loss of lithium-ion batteries to reflect the lithium-ion batteries capacity degradation process.

The data-driven methods use the characteristics extracted from the battery degradation data that can reflect the law of battery degradation to perform RUL prediction. Shen et al. [14] proposed a cell-level capacity estimation method based on Deep Convolutional Neural Network, which uses the measured value during charging to estimate the battery capacity. Wang et al. [15] proposed a method using artificial bee colony and support vector regression to improve the RUL prediction accuracy of LIBs. Wang et al. [16] proposed a method for the remaining useful life of lithium-ion batteries is proposed, which is based on support vector regression and differential evolution. The experimental data considers the capacity, voltage and current during discharge operation. Zhao et al. [17] established the relationship model between HIS and capacity by combining the feature vector selection and support vector regression, so as to evaluate online capacity and make SOH and RUL more accurate prediction. Ma et al. [18] combined the idea of Broad Learning and proposed Broad Learning-Extreme Learning Machine model. And three different data sets are used to estimate the battery state. Guo et al. [19] proposed a data-driven method for estimating the remaining capacity of lithium-ion batteries based on the extraction of charging health feature. In order to adapt to different working conditions, health features are extracted and optimized through rational analysis and principal component analysis. The relevance vector machine is used to estimate capacity. Fan et al. [20] proposed a hybrid neural network based on gate recurrent unit-convolutional neural network to estimate SOH, and used two different data sets for verification.

It can be found from the above research that the existing experimental results are mostly obtained by using the long-term degradation data of lithium-ion batteries, while the research on the lithium-ion batteries early cycle data is rarely mentioned. Kristen A. et al. [21] used the lithium-ion battery data of the first 100 cycles for feature extraction and generated three different linear models to predict the battery life. The model with the best result used nine features and achieved a test error of 9.1%. However, the characteristic data of lithium-ion batteries is often non-linear due to the complex internal degradation process and many influencing factors. There are still many difficulties in accurately predicting with a single linear model.

Neural networks can be used to solve non-linear problems and are widely used to the remaining useful life prediction of lithium-ion batteries. LSTM can be used to deal with non-linear problems and time series problems. Bian et al. [22] proposed a stacked bidirectional long short-term memory neural network which is used to estimate state of charge. Fasahat et al. [23] proposed a method of combining autoencoder neural network with Long Short-Term Memory neural network which is used to improve the estimation accuracy of battery SOC. Li et al. [24] proposed a remaining useful life prediction hybrid method which is combined the empirical model decomposition algorithm with long short-term memory and Elman neural networks. Li et al. [25] proposed a AST-LSTM model which is a variant long-short-term memory neural network. Experiments are performed on capacity estimation and remaining useful life prediction using NASA data. LSTM has a good effect in time series prediction and can effectively solve the long-term dependence problem through gated structure.

However, the degradation characteristics of the early battery cycle data are not obvious. If the original data is directly input into the neural network, the characteristic information is often not effectively captured. Broad Learning System (BLS) is a neural network structure which does not depend on the depth structure. Its predecessor is random vector functional-link neural network (RVFLNN). BLS can expand the original input data into more effective feature vectors and using BLS to process the early cycle data can better obtain the effective information in the early cycle data and effectively improve the prediction accuracy.

Therefore, this paper proposes a LSTM method that combines the idea of BLS, called BLS-LSTM, and uses the early cycle data to predict the remaining useful life of lithium-ion batteries. Firstly, the method generates feature nodes through mapping operation on early data features, and then generates enhancement nodes through enhancement operation on feature nodes. Secondly, new input nodes are obtained by combining feature nodes and enhancement nodes and taken as the new input layer. Finally, the prediction results are obtained through LSTM. This method avoids the problem that the effective features of input data can not be captured, and the prediction effect of single linear model on complex input data is not good. The experimental results of the proposed method compared with Ref. [21] and other existing methods show that BLS-LSTM is more effective in predicting the remaining useful life of batteries using early cycle data.

The rest of this paper is as follows: Section 2 introduces the principle of BLS, LSTM and BLS-LSTM. Section 3 introduces the experimental data and results, and compares BLS-LSTM with other methods. Section 4 is conclusion.

II. Methodology

A. Broad Learning System

Broad learning system (BLS) [26] is a kind of neural network structure independent of depth structure. Its predecessor is RVFLNN. Firstly, BLS performs mapping operations on input data to generate mapping features that form a valid representation of the input data. Then, the enhanced nodes are obtained by enhancing the mapping features. Finally, the new input nodes are obtained by combining feature nodes and enhancement nodes and directly connected to output layer, the output weights are calculated by ridge regression. The Broad Learning System is shown in Fig. 1.

B. Long Short-Term Memory

Recurrent Neural Networks (RNN) can process sequence data related to the input before and after because of its memory

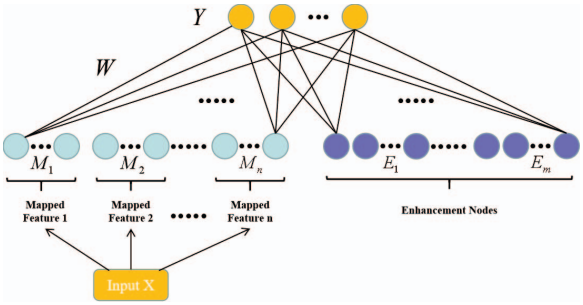

Fig. 1. The structure of Broad Learning System.

characteristics, so it is widely used in the field of natural language processing and various time series predictions. However, the disappearance of gradients or the phenomenon of gradient explosions make RNN unable to capture long-term dependence in traditional back propagation training [27]. Therefore, the gating algorithm is used to solve this problem. The idea is that the gating unit gives the recurrent neural network with the ability to control the accumulation of internal information, which can not only master the long-distance dependence but also selectively forget the information to prevent overload.

LSTM [28] is the earliest proposed recurrent neural network gating algorithm, and its corresponding recurrent unit contains three gates which are input gate, forget gate and output gate [29]. LSTM can ease the problem of gradient disappearance by combining short-term memory with long-term memory through "gate" structure. The LSTM structure is shown in Fig. 2.

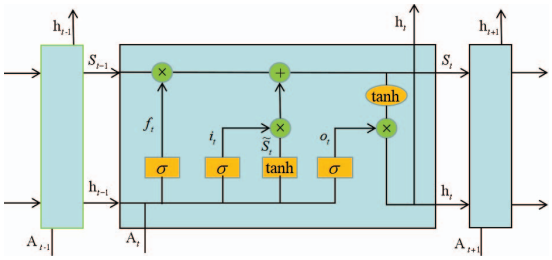

Fig. 2. The structure of LSTM.

C. BLS-LSTM

In this paper, the BLS-LSTM network structure is constructed. The BLS-LSTM structure is shown in Fig. 3. BLS performs feature mapping and feature enhancement on the input data, so that more effective feature information can be obtained from the input data. The problem of not being able to effectively capture the features of the original input data is avoided. And LSTM can effectively solve the problem of long-term dependence and has a good performance in time series forecasting. Firstly, BLS-LSTM maps the input data to

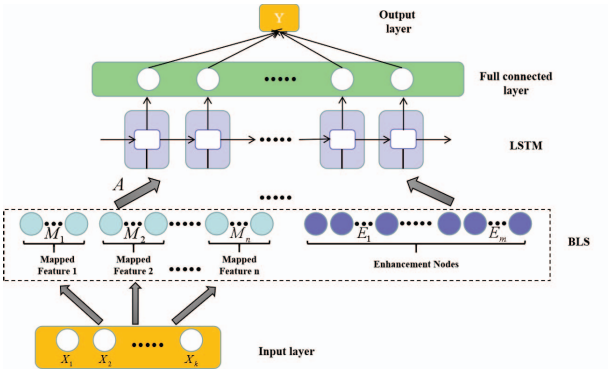

Fig. 3. The structure of BLS-LSTM.

obtain *n* sets of mapping features, each of which has *p* nodes. The calculation formula is as follows:

$$M_i = \phi_i(XW_{Mi} + \beta_{Mi}), i = 1, 2, ..., n \tag{1}$$

where *i* represents the *i*-th group of mapping features, *X* is the input data, W_{Mi} and β_{Mi} are random weights and biases with appropriate dimensions, respectively. All mapping nodes are represented as follows: $M^n = [M_1, M_2, ..., M_n]$.

Then, according to the mapping features, the enhancement nodes are obtained which have m groups with *q* nodes in each group. The calculation formula is as follows:

$$E_j = \varphi_j(M^n W_{ej} + \beta_{ej}), j = 1, 2, ..., m \tag{2}$$

where *j* represents the *j*-th group of enhancement nodes. All enhancement nodes are represented as follows: $E^m = [E_1, E_2, ..., E_m]$. In practice, different values of *p*, *q*, *n* and *m* can be selected according to different tasks. In addition, when $i \neq k$, ϕ_i and ϕ_k can be different functions. Similarly, when $j \neq l$, φ_j and φ_l can be different functions.

Next, new input nodes are obtained by combining the mapping nodes and the enhancement nodes. The calculation formula is as follows:

$$A = [M^n | E^m] \tag{3}$$

Input the new input nodes $A = [A_1, A_2, ..., A_k]$ into LSTM to enter into forget gate, input gate and output gate. Forget gate controls the amount of information that can be passed from the previous moment to the current moment, and outputs a value between 0 and 1 that determines how much historical information to forget. The calculation formula of forget gate is as follows:

$$f_t = \sigma(W_f \cdot [h_{t-1}, A_t] + b_f) \tag{4}$$

where h_{t-1} is the hidden state of the previous moment, A_t is the input of the current moment, the weight and bias of the forget gate are represented by W_f and b_f respectively.

Input gate controls the amount of information that can be saved to the unit state at the current moment. The sigmoid layer can determines which value can be updated, is called

"input gate layer". The calculation formula of input gate is as follows:

$$i_t = \sigma(W_i \cdot [h_{t-1}, A_t] + b_i) \tag{5}$$

where the weight and bias of the input gate are represented by W_i and b_i respectively. Then a new candidate value vector $\widetilde{S}_t$ is created by a tanh layer which can be added to the state.

$$\widetilde{S}_t = tanh(W_c \cdot [h_{t-1}, A_t] + b_c) \tag{6}$$

where W_c and b_c represent the weight and bias of candidate value vector.

Output gate determines the amount of information that the unit state can output to the current state output value, represented by o_t.

$$S_t = f_t * S_{t-1} + i_t * \widetilde{S}_t \tag{7}$$

$$o_t = \sigma(W_o \cdot [h_{t-1}, A_t] + b_o) \tag{8}$$

$$h_t = o_t * tanh(S_{t-1}) \tag{9}$$

where the weight and bias of the output gate are represented by W_o and b_o respectively, S_t is the current unit state, h_t is the updated hidden state.

Finally, the output h_t of each time is connected with the full connection layer to get the final result.

The framework of BLS-LSTM is shown in Fig. 4. Firstly, feature extraction is carried out for the original data. Then the extracted features are mapped and enhanced to obtain new input nodes and input them into the LSTM for prediction. Finally, the prediction results are obtained.

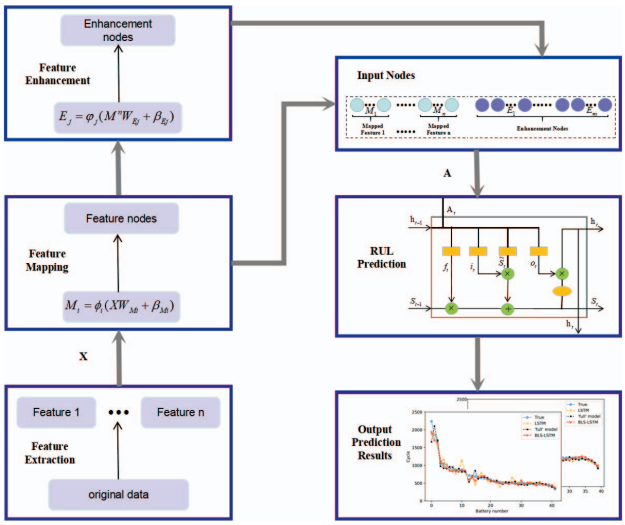

Fig. 4. The framework of BLS-LSTM.

III. Experiments and Discussion

A. Experimental data

In this paper, the data of experiment comes from the data set provided by the Ref. [21]. Commercial LFP/graphite cells were used to cycle in a constant temperature environmental chamber (30°C) under different fast-charging conditions but the same discharging conditions, and finally generated a data set of 124 cells. The data set contains cycle life of different lengths, the maximum is 2300 cycles, the minimum is 150 cycles. During the cycle, the device continuously measured voltage, current, battery temperature and internal resistance, and the data set contains approximately 96700 cycles [21].

The experiment is to use early cycle data to predict the life of lithium-ion batteries. The data of the first 100 cycles, the first 80 cycles and the first 60 cycles of the battery are respectively analyzed, and $\Delta Q_{i-10}(V)$ is obtained from the discharge voltage curve $Q(V)$, $\Delta Q_{i-10}(V) = Q_i(V) - Q_{10}(V)(i = 100, 80, 60)$, i represents the discharge voltage curve of the i-th cycle. Ref. [21] extracted 20 features from $\Delta Q_{100-10}(V)$, discharge capacity decay curve features, and other features including temperature and charging time. The full model, which has the best prediction results, uses nine of the features to predict. Ref. [21] divides 124 battery data into three parts, 41 battery data as training set, 43 battery data as primary testing set for model performance evaluation, and 40 battery data as secondary testing set for model evaluation.

In this experiment, 41-43-40 data set classification method is also selected for training and prediction. The minimum value, skewness, kurtosis and variance of $\Delta Q_{i-10}(V)$, slope of linear fit to the capacity fade curve from cycles 2 to i, internal resistance difference between i-th cycle and 2nd cycle, the discharge capacity of 2nd cycle, the average charge time of the first 5 times, and the difference between max discharge capacity and 2nd cycle are selected as input data for BLS-LSTM. The final experimental results are compared with Ref. [21].

In order to illustrate the effectiveness of the selected features, the Gray Relation Analysis (GRA) is used to calculate the correlation between the selected features and the battery life. Fig. 5 is the gray correlation diagram between 9 features selected from the first 100 cycles data and battery life. It can be seen from the figure that the correlation between the selected features and battery life is all above 0.7. It shows that the 9 features extracted from the early battery degradation data can effectively predict the battery remaining useful life.

B. Evaluation criteria

This article chooses the same evaluation indicators as Ref.[21] to evaluate the model, namely Root Mean Squared Error (RMSE) and mean percentage error (%err). The calculation formula is as follows:

$$RMSE = \sqrt{\frac{1}{m}\sum_{i=1}^{m}(y_i - \hat{y}_i)^2} \tag{10}$$

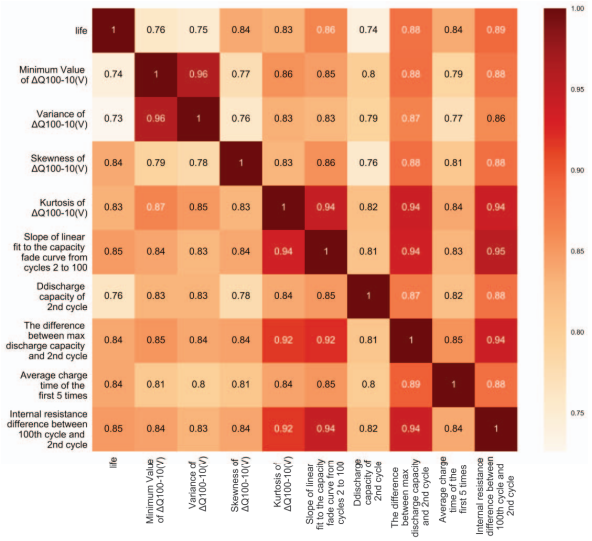

Fig. 5. Gray correlation between 9 features selected from the first 100 cycles data and battery life.

$$\%err = \frac{1}{m}\sum_{i=1}^{m}\left|\frac{y_i - \hat{y}_i}{y_i}\right| \times 100 \tag{11}$$

where the total number of sample data is represented by m, the true cycle life of the battery is represented by y_i, and the prediction value of battery cycle life is represented by $\hat{y}_i$.

1) The prediction with the first 100 cycles data: In this section, BLS-LSTM uses data from the first 100 cycles of the battery for prediction, and the experimental results are compared with other methods. The prediction results of BLS-LSTM, "full" model and LSTM are shown in Fig. 6. The batteries are sorted according to the cycle life to better display the prediction results. Fig. 6a and Fig. 6b are the prediction results on the primary test set and the secondary test set, respectively. In the figure, the blue dots represent the true values, the red dots represent the BLS-LSTM predicted values, the black dots represent the "full" model predicted values, and the yellow dots represent the LSTM predicted values. It can be seen from the figure that the red point is closer to the blue point, that is, the predicted value of BLS-LSTM is closer to the true value, which reflects the accuracy of the proposed method.

The box-plot comparison of the predicted percentage error of BLS-LSTM, "full" model and LSTM on the primary test set and secondary test set are shown in Fig. 7, which can show the distribution of prediction error, and the ordinate represents the predicted percentage error. The two ends of the box correspond to the upper and lower quartiles of the data. The narrower the box means the more concentrated the data, the lower position of the box means the smaller the value of the data. The points outside the box represent discrete points. As can be seen from Fig. 7, BLS-LSTM has the smallest box, low position and small value of discrete points on the primary test set and secondary test set. The box of LSTM is the largest, the position is high, and the value of discrete points is large. It shows that the prediction result of BLS-LSTM is superior to the "full" model and LSTM, which reflects the effectiveness and generalization ability of the proposed method, and also shows that the introduction of BLS can achieve higher prediction accuracy.

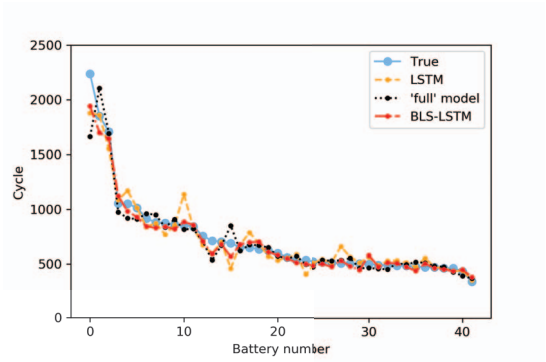

(a) Primary test

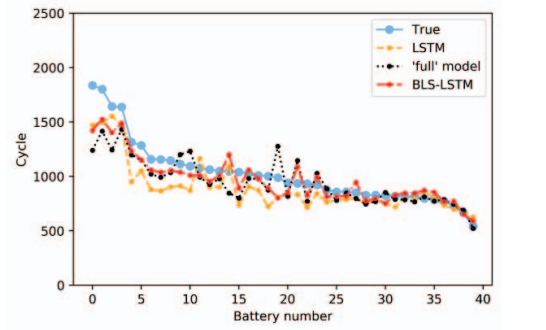

(b) Secondary test

Fig. 6. The prediction result.

Table 1 tabulates the experimental results of BLS-LSTM and other methods. In the primary test set, there is a battery quickly reached an 80% state of health which did not match the degradation trend of other batteries. Therefore, the results of excluding the battery are shown in brackets [21]. It can be seen that after the removal of abnormal battery, the average error of BLS-LSTM is 7.6%, and the average error of full model is 9.1%. The accuracy of BLS-LSTM is superior to "full" model. Compared with LSTM, the average error of BLS-LSTM is reduced by 4%, which indicates the effectiveness of feature extension by BLS. Through comparison, it is found that the experiment results of BLS-LSTM are better than other models, indicating that BLS-LSTM has better performance and better generalization ability in predicting RUL of the battery using early cycle data.

In order to discuss the influence of data set partition on the prediction results, the training set and test set are re-divided. On the premise of not removing the abnormal battery, the training set is 70% of the data, and the test set is 30% of the data. Fig. 8 shows the comparison between BLS-LSTM and

TABLE I
COMPARISON OF BLS-LSTM AND OTHER METHODS.

Algorithm	RMSE(cycle)			Mean percent error(%)		
	Train	Prim.Test	Sec.Test	Train	Prim.Test	Sec.Test
"full" model	51	118(100)	214	5.6	14.1(7.5)	10.7
MLP	56	141(132)	160	6.1	12.3(10.2)	11.3
SVR	84	122(90)	141	6.3	15.5(10.6)	9.0
LSTM	94	108(102)	173	10.6	12.6(10.8)	12.9
BLS-LSTM	40	98(73)	120	3.8	11.1(6.5)	8.6

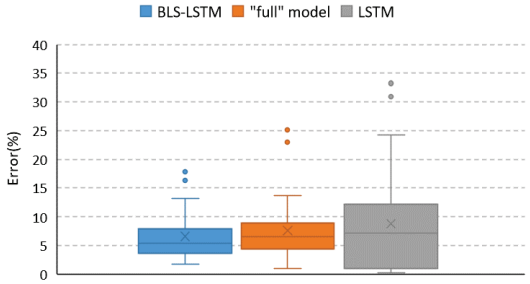

(a) Primary test

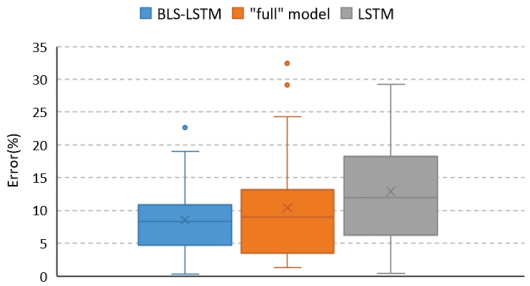

(b) Secondary test

Fig. 7. The box-plot comparison of the predicted percentage error.

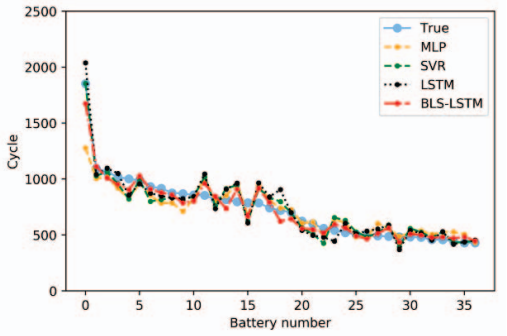

(a) The prediction results.

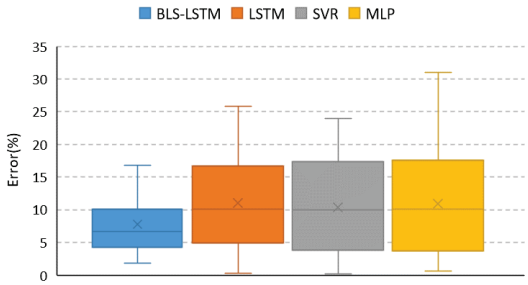

(b) The box-plot comparison.

Fig. 8. The comparison of prediction results.

other methods. Fig. 8a shows the prediction results of BLS-LSTM and other methods on the new test set, and Fig. 8b shows the box-plot of the prediction percentage error. It can be seen from the Fig. 8b that the BLS-LSTM has the smallest box and the most concentrated data. 75% of the prediction errors are below 10%, which further illustrates the proposed model has a good prediction result.

Table 2 tabulates the prediction results of different methods after re-dividing the data set. From the table, it can be seen that the RMSE and mean percent error of BLS-LSTM are 67 and 8.1%, respectively, which are smaller than other methods, indicating that the model has more good generalization ability and effectiveness. The mean percent error of the "full" model without removing the abnormal battery is 12.4%. After re-dividing the data set, the prediction results of the proposed

TABLE II
THE PREDICTION RESULTS OF BLS-LSTM AND OTHER METHODS.

Algorithm	RMSE(cycles)		Mean percent error(%)	
	Train	Test	Train	Test
MLP	60	120	6.3	10.9
SVR	72	88	6.9	10.3
LSTM	87	96	9.7	11.1
BLS-LSTM	53	67	5.1	8.1

TABLE III
COMPARISON OF PREDICTION RESULTS USING DIFFERENT EARLY CYCLE DATA.

Algorithm	Start point	RMSE(cycle)			Mean percent error(%)		
		Train	Prim.Test	Sec.Test	Train	Prim.Test	Sec.Test
BLS-LSTM	100	40	98(73)	120	3.8	11.1(6.5)	8.6
	80	68	101(96)	139	5.9	13.0(7.3)	9.7
	60	62	123(128)	170	6.3	15.9(11.0)	13.1
"full" model	100	51	118(100)	214	5.6	14.1(7.5)	10.7

method are all smaller than 12.4%. The results show that the data set partition method will have an impact on the experimental results, and the network training with more data can get better results. The effectiveness of the proposed method is verified.

2) The prediction with other early cycles data: In order to further illustrate the effectiveness of BLS-LSTM in early life prediction, the data features of the first 80 cycles and the first 60 cycles are used to predict the battery cycle life (denoted as BLS-LSTM(80) and BLS-LSTM(60)), and compared with the prediction results of the BLS-LSTM and the "full" model using the data of the first 100 cycles (denoted as BLS-LSTM(100) and "full" model(100)). Fig. 9 is a box-plot of the prediction error percentage. Fig. 9a shows that on the primary test set, the BLS-LSTM(100) has the smallest box, the lowest position, and the discrete points closest to the box, indicating that the BLS-LSTM(100) has the best prediction results. Although the box of BLS-LSTM(60) is small, its position is higher than the other three boxes, and there are three discrete points, which shows that the prediction result of BLS-LSTM(60) is the worst. Similarly, Fig. 9b shows that on the secondary test set, BLS-LSTM(100) has the best result and BLS-LSTM(60) has the worst result. The Table 3 shows the statistical results. As show in the table, the average test error of BLS-LSTM(80) is 8.5%, which is still better than the result of "full" model(100), indicating that the proposed model has higher accuracy and effectiveness in early life prediction. And the average test error of BLS-LSTM(60) is 12.1%, the result is the worst. The main reason for this result is that the degradation trend is less obvious with the earlier the cycle data, the less effective information can be captured from it, and accordingly, the prediction accuracy will also decrease.

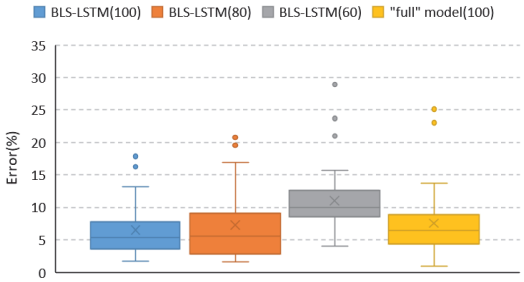

(a) Primary test

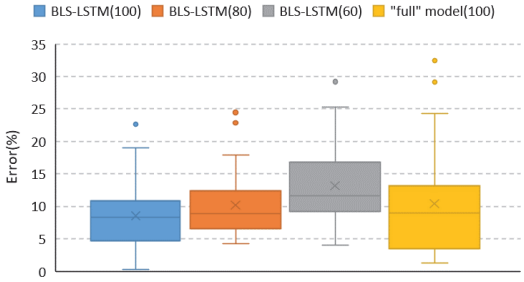

(b) Secondary test

Fig. 9. The box-plot comparison of the predicted percentage error.

IV. CONCLUSIONS

This paper proposes BLS-LSTM model which use early cycle data to accurately predict the remaining useful life of lithium-ion batteries. Firstly, the model performs feature mapping operation on input data to generate feature nodes. Secondly, the enhancement operation is preformed on feature nodes to generate enhanced nodes. Finally, the feature nodes and the enhancement nodes are combined as the new input nodes, and the new input nodes are input into the LSTM to predict the remaining useful life of lithium-ion batteries. The experiment uses different early cycle data to predict the remaining useful life, and the experimental results are compared with "full" model and other methods. They show that the average prediction errors of BLS-LSTM are 7.8% and 8.5% when using the first 100 cycles and the first 80 cycles, respectively, which are higher than "full" model. This reflects the effectiveness of the proposed method in early life prediction. This article also re-divides the training set and test set of the first 100 cycles of data. Without removing the abnormal battery, experiment set 70% of the data as the training set and the rest as the test set. The experimental results show that the average prediction error of BLS-LSTM is 8.1%, which is smaller than other methods. It shows that using more training data can get better prediction results, and further illustrates the accuracy and effectiveness of the proposed method in the prediction of remaining useful life using early data.

ACKNOWLEDGMENT

This research is supported by the National Natural Science Foundation of China (No.61873175), and Academy for Multidisciplinary Studies of Capital Normal University, and Youth Innovative Research Team of Capital Normal University. Corresponding author: Lifeng Wu.

REFERENCES

[1] Q. Zhu, M. Xu, W. Liu, and M. Zheng, "A state of charge estimation method for lithium-ion batteries based on fractional order adaptive extended kalman filter," Energy, vol. 187, p. 115880, 2019.

[2] M. Kim et al., "Data-efficient parameter identification of electrochemical lithium-ion battery model using deep Bayesian harmony search," Applied Energy, vol. 254, no. August, p. 113644, 2019.

[3] G. Ma, Y. Zhang, C. Cheng, B. Zhou, and Y. Yuan, "Remaining useful life prediction of lithium-ion batteries based on false nearest neighbors and a hybrid neural network," Applied Energy, vol. 253, 2019.

[4] K. Khodadadi Sadabadi, X. Jin, and G. Rizzoni, "Prediction of remaining useful life for a composite electrode lithium ion battery cell using an electrochemical model to estimate the state of health," Journal of Power Sources, vol. 481, no. April 2020, p. 228861, 2021.

[5] X. Qiu, W. Wu, and S. Wang, "Remaining useful life prediction of lithium-ion battery based on improved cuckoo search particle filter and a novel state of charge estimation method," Journal of Power Sources, vol. 450, no. November 2019, p. 227700, 2020.

[6] L. O. Avila, M. L. Errecalde, F. M. Serra, and E. C. Martinez, "State of charge monitoring of Li-ion batteries for electric vehicles using GP filtering," Journal of Energy Storage, vol. 25, no. August, p. 100837, 2019.

[7] W. Li et al., "Electrochemical model-based state estimation for lithium-ion batteries with adaptive unscented Kalman filter," Journal of Power Sources, vol. 476, no. May, 2020.

[8] H. Zhang, Z. Mo, J. Wang, and Q. Miao, "Nonlinear-drifted fractional brownian motion with multiple hidden state variables for remaining useful life prediction of lithium-ion batteries," IEEE Transactions on Reliability, vol. 69, no. 2, pp. 768-780, 2020.

[9] Y. Ma, Y. Chen, X. Zhou, and H. Chen, "Remaining Useful Life Prediction of Lithium-Ion Battery Based on GaussCHermite Particle Filter," IEEE Transactions on Control Systems Technology, vol. 27, no. 4, pp. 1788-1795, 2019.

[10] H. Yang, X. Sun, Y. An, X. Zhang, T. Wei, and Y. Ma, "Online parameters identification and state of charge estimation for lithium-ion capacitor based on improved Cubature Kalman filter," Journal of Energy Storage, vol. 24, no. June, p. 100810, 2019.

[11] Y. Zhang, R. Xiong, H. He, and M. G. Pecht, "Lithium-Ion Battery Remaining Useful Life Prediction With BoxCCox Transformation and Monte Carlo Simulation," IEEE Transactions on Industrial Electronics, vol. 66, no. 2, pp. 1585-1597, 2019.

[12] H. Zhang, Q. Miao, X. Zhang, and Z. Liu, "An improved unscented particle filter approach for lithium-ion battery remaining useful life prediction," Microelectronics Reliability, vol. 81, no. 24, pp. 288-298, 2018.

[13] F. Yang, X. Song, G. Dong, and K. L. Tsui, "A coulombic efficiency-based model for prognostics and health estimation of lithium-ion batteries," Energy, vol. 171, pp. 1173-1182, 2019.

[14] S. Shen, M. Sadoughi, X. Chen, M. Hong, and C. Hu, "A deep learning method for online capacity estimation of lithium-ion batteries," Journal of Energy Storage, vol. 25, no. June, p. 100817, 2019.

[15] Y. Wang, Y. Ni, S. Lu, J. Wang, and X. Zhang, "Remaining Useful Life Prediction of Lithium-Ion Batteries Using Support Vector Regression Optimized by Artificial Bee Colony," IEEE Transactions on Vehicular Technology, vol. 68, no. 10, pp. 9543-9553, 2019.

[16] F. K. Wang and T. Mamo, "A hybrid model based on support vector regression and differential evolution for remaining useful lifetime prediction of lithium-ion batteries," Journal of Power Sources, vol. 401, no. March, pp. 49-54, 2018.

[17] Q. Zhao, X. Qin, H. Zhao, and W. Feng, "A novel prediction method based on the support vector regression for the remaining useful life of lithium-ion batteries," Microelectronics Reliability, vol. 85, no. jun., pp. 99-108, 2018.

[18] Y. Ma, L. Wu, Y. Guan, and Z. Peng, "The capacity estimation and cycle life prediction of lithium-ion batteries using a new broad extreme learning machine approach," Journal of Power Sources, vol. 476, no. 56, p. 228581, 2020.

[19] P. Guo, Z. Cheng, and L. Yang, "A data-driven remaining capacity estimation approach for lithium-ion batteries based on charging health feature extraction," Journal of Power Sources, vol. 412, pp. 442-450, 2019.

[20] Y. Fan, F. Xiao, C. Li, G. Yang, and X. Tang, "A novel deep learning framework for state of health estimation of lithium-ion battery," Journal of Energy Storage, vol. 32, no. June, p. 101741, 2020.

[21] K. A. Severson et al., "Data-driven prediction of battery cycle life before capacity degradation," Nature Energy, vol. 4, no. 5, pp. 383-391, 2019.

[22] C. Bian, H. He, and S. Yang, "Stacked bidirectional long short-term memory networks for state-of-charge estimation of lithium-ion batteries," Energy, vol. 191, p. 116538, 2020.

[23] M. Fasahat and M. Manthouri, "State of charge estimation of lithium-ion batteries using hybrid autoencoder and Long Short Term Memory neural networks," Journal of Power Sources, vol. 469, no. January, p. 228375, 2020.

[24] X. Li, L. Zhang, Z. Wang, and P. Dong, "Remaining useful life prediction for lithium-ion batteries based on a hybrid model combining the long short-term memory and Elman neural networks," Journal of Energy Storage, vol. 21, no. November 2018, pp. 510-518, 2019.

[25] P. Li et al., "State-of-health estimation and remaining useful life prediction for the lithium-ion battery based on a variant long short term memory neural network," Journal of Power Sources, vol. 459, no. October 2019, p. 228069, 2020.

[26] C. L. P. Chen and Z. Liu, "Broad Learning System: An Effective and Efficient Incremental Learning System Without the Need for Deep Architecture," IEEE Transactions on Neural Networks and Learning Systems, vol. 29, no. 1, pp. 10-24, 2018.

[27] Y. Bengio, P. Simard, and P. Frasconi, "Learning long-term dependencies with gradient descent is difficult," Neural Networks, IEEE Transactions on, 1994.

[28] S. Hochreiter and J. Schmidhuber, "Long Short-Term Memory," Neural Computation, vol. 9, no. 8, pp. 1735-1780, 1997.

[29] Y. Tian, R. Lai, X. Li, L. Xiang, and J. Tian, "A combined method for state-of-charge estimation for lithium-ion batteries using a long short-term memory network and an adaptive cubature Kalman filter," Applied Energy, vol. 265, no. November 2019, p. 114789, 2020.